Insertion Loop 256−268 in Coagulation Factor IX Restricts Enzymatic Activity in the Absence but Not in the Presence of Factor VIII[†]

Joost A. Kolkman[‡] and Koen Mertens*[,‡,§]

Department of Plasma Proteins, CLB, Amsterdam, The Netherlands, and Department of Pharmaceutics, Utrecht Institute for Pharmaceutical Sciences (UIPS), Utrecht University, Utrecht, The Netherlands

Received November 29, 1999; Revised Manuscript Received March 7, 2000

ABSTRACT: Insertions in surface loops bordering the substrate-binding groove have been shown to play a major role in the interaction of serine proteases with their cognate inhibitors and substrates. In the present study, we investigated the functional role of factor IX insertion loop 256−268, and in particular of residues Asn^{264} and Lys^{265} therein. To this end, the purified and activated mutants des-(N264,K265)-FIX and FIX-K265A were compared to normal factor IXa with regard to a number of functional properties. The catalytic efficiency of des-(N264,K265)-FIXa and FIXa-K265A toward the amide substrate CH_3SO_2-Leu-Gly-Arg-pNA was 2−3-fold increased relative to that of normal factor IXa. Comparison of the activities of normal and mutant factor IXa toward a series of closely related amide substrates indicates that mutation of residues Asn^{264}−Lys^{265} influences the interactions in the S2-binding site. The mutations in loop 256−268 also increased the susceptibility of factor IXa to antithrombin inhibition by approximately 3-fold. Factor X activation experiments in the absence of factor VIIIa revealed that the catalytic efficiency of des-(N264,K265)-FIXa and FIXa-K265A was about 20 times higher than that of normal factor IXa. In the presence of factor VIIIa, however, the activity toward factor X was similar to that of normal factor IXa. The reduced sensitivity of the factor IXa mutants to factor VIIIa was neither due to an increase in factor IXa-dependent inactivation of factor VIIIa, nor to a lower affinity for this cofactor. Overall, these data demonstrate that loop 256−268 restricts the activity of factor IXa toward both synthetic and natural substrates. Complex formation with factor VIIIa alleviates the inhibitory effect of this insertion loop on the activation of FX.

Human factor IX (FIX)[1] is a vitamin K dependent protein that circulates in plasma as a precursor of a serine protease. FIX consists of an N-terminal γ-carboxyglutamic acid (Gla) domain, followed by a short hydrophobic sequence, two epidermal growth factor (EGF)-like domains, an activation peptide, and the C-terminal protease domain (*1*, *2*). During the coagulation process, FIX is activated by cleavage of two peptide bonds, Arg^{145}−Ala^{146} and Arg^{180}−Val^{181}, by either factor XIa (FXIa) or the membrane-bound factor VIIa−tissue factor complex (*3*). Activated FIX (FIXa) then activates factor X (FX) into FXa, a process which requires calcium ions, a membrane surface, and a nonenzymatic cofactor, factor VIIIa (FVIIIa) (*4*). The importance of FIX in hemostasis is apparent from the notion that a deficiency or a functional defect in FIX is associated with the bleeding disorder hemophilia B. In comparison with other coagulation enzymes, such as FXa and thrombin, FIXa exhibits extremely low intrinsic activity toward natural and synthetic substrates. Complex formation with FVIIIa overcomes this limitation and results in an enormous increase in FX activation (*5*, *6*). By contrast, FVIIIa has little or no effect on the catalytic activity of FIXa toward synthetic peptide substrates (*7*, *8*).

Recently, we have demonstrated that two surface-exposed structure elements in the FIXa protease domain, i.e., α-helix 333−339 and loop 199−204, play important but distinct roles in the enzymatic activity of FIXa (*9*, *10*). The former region appears to be involved in the FVIIIa-dependent stimulation of FIXa activity, while the latter contributes to macromolecular substrate and inhibitor recognition. Loop 199−204 is one of six surface loops that constitute the substrate-binding groove in FIX. Previous studies for a number of serine proteases have shown that insertions in these surface loops may be important structural determinants of enzyme activity and/or substrate specificity. For example, in thrombin residues Tyr^{367}−Trp^{370} [*c*60A−60D] and Glu^{466}−Trp^{468} [*c*146−148] (chymotrypsinogen numbering in brackets), located in the so-called B- and C-insertion loops, respectively, play a crucial role in the reactivity toward various serine protease inhibitors and substrates (*11*, *12*). In addition, residues located in insertion 296−302 [*c*36−37E] of tissue-type plasminogen activator modulate the interaction with its

[†] This research was supported by the Netherlands Organization for Scientific Research (NWO) (Grant 902-26-152).

* To whom correspondence should be addressed at CLB, Department of Plasma Proteins, Plesmanlaan 125, 1066 CX Amsterdam, The Netherlands. Tel.: +31-20-5123120. Fax: +31-20-5123680. Email: k_mertens@clb.nl.

[‡] CLB.

[§] UIPS.

[1] Abbreviations: FIX, factor IX; FIXa, activated factor IX; FVIII, factor VIII; FVIIIa, activated FVIII; FXIa, activated factor XI; FX, factor X; FXa, activated factor X; CH_3SO_2-LGR-pNA, CH_3SO_2-D-leucyl-L-glycyl-L-arginyl-*p*-nitroanilide; DMEM, Dulbecco's modified Eagle's medium; MDCK, Madin−Darby canine kidney; PAGE, polyacrylamide gel electrophoresis; HSA, human serum albumin; FCS, fetal calf serum.

10.1021/bi992735q CCC: $19.00
Published on Web 05/31/2000

Table 1: Sequence Alignment of Human FIX Region 256−269 and the Corresponding Regions of Related Serine Proteases[a]

	256[*c*91]	269[*c*102]
factor IX	H H N Y N A A I [N K] Y N H **D**	
factor VII	P S T Y V P G T · · T N H **D**	
factor X	H N R F T K E T · · Y D F **D**	
protein C	H P N Y S K S T · · T D N **D**	
prothrombin	H P R Y N W R E N · L D R **D**	
trypsin	H P S Y N S N T · · L N N **D**	

[a] Sequence alignment of human factor IX region 256−269 and the corresponding regions of human factor VII, factor X, protein C, prothrombin, and bovine trypsin. Catalytic triad residue Asp^{269} is indicated in boldface type. Chymotrypsinogen numbering is indicated in brackets. Residues Asn^{264} and Lys^{265} are boxed.

physiological inhibitor plasminogen activator inhibitor type 1 (*13*). Interestingly, comparison of FIX with other coagulation proteases reveals that one of its surface loops, comprising residues 256−268 [*c*91−101], contains a unique insertion of two residues (see Table 1). We speculated that this insertion loop might be underlying FIXa's low catalytic activity toward synthetic and natural substrates. This view would be in line with the observation that replacement of residues 260−265 by the corresponding FX sequence (NAAINK→TKET) in a FIXa variant lacking both the Gla and EGF1 domains promoted the reactivity toward two different amide substrates (*14*). However, the role of insertion loop 256−268 in the activity of complete, full-length FIXa toward its natural substrate FX and the FVIIIa-dependent stimulation thereof have remained unresolved. In the present study, we addressed this issue by functional analysis of FIXa variants with mutations in loop 256−268. The Asn^{264}−Lys^{265} motif within this region was selected for mutagenesis, because it comprises residues with relatively large side chains that are fully exposed to solvent (*15*, *16*). Moreover, this motif is unique to FIX and completely conserved in the nine FIX sequences known to date (*17*). The FIX variants were expressed in mammalian cells, purified by immunoaffinity chromatography, and subsequently activated by FXIa. The activated mutants were compared to normal FIXa with respect to a number of functional parameters, including the reactivity toward antithrombin and the natural substrate FX. This approach revealed that insertion loop 256−268 is a major structural determinant of FIXa activity in the absence of FVIIIa, but not in the presence of this cofactor.

EXPERIMENTAL PROCEDURES

Materials. The Thermo Sequenase cycle sequencing kit, CNBr−Sepharose CL4B, and Q-Sepharose FF were from Amersham Pharmacia Biotech Benelux (Roosendaal, The Netherlands). L-α-Phosphatidyl-L-serine and L-α-phosphatidylcholine were obtained from Sigma. Dulbecco's modified Eagle's medium (DMEM), fetal calf serum (FCS), oligonucleotide primers, restriction enzymes, and DNA modifying enzymes were purchased from Life Technologies (Breda, The Netherlands). *Pfu*-polymerase was obtained from Stratagene (Cambridge, U.K.). CH_3SO_2-D-leucyl-glycyl-arginyl-*p*-nitroanilide (CH_3SO_2-LGR-pNA), product name CBS 31.39, was purchased from Diagnostica Stago (Asnières, France). CH_3OCO-D-cyclohexylglycyl-glycyl-arginyl-*p*-nitroanilide (CH_3OCO-CHG-Gly-Arg-pNA) was obtained from Dade Behring. CH_3OCO-D-cyclohexylglycyl-norvalyl-arginyl-*p*-nitroanilide (CH_3OCO-CHG-NVal-Arg-pNA), H-D-cyclohexylglycyl-norvalyl-arginyl-*p*-nitroanilide (H-CHG-NVal-Arg-pNA), and CH_3OCO-D-cyclohexyltyrosyl-norvalyl-arginyl-*p*-nitroanilide (CH_3OCO-CHT-NVal-Arg-pNA) from Pentapharm (Basel, Switzerland) were generously provided by C. Kortmann from Kordia B. V. (Leiden, The Netherlands).

Proteins. The monoclonal anti-FIX antibody CLB-FIX 14 has been described previously (*18*). Polyclonal antibodies against FIX were obtained as described (*19*). Plasma-derived FIX (pd-FIX) was prepared as described elsewhere (*20*). FXIa was obtained from Enzyme Research Laboratories (South Bend, IN). FVIII was purified as outlined previously (*19*). FX was purified as described (*21*). Purified antithrombin and human serum albumin (HSA) were from the Division of Products of CLB, Amsterdam, The Netherlands. Purified FVIIIa was obtained as described by Curtis et al. (*22*). FVIII A2 subunit was isolated from FVIIIa by mono S chromatography as described by Fay et al. (*23*).

Protein Concentrations. FIX antigen was measured by enzyme-linked immunosorbent assay employing a previously described method (*20*). Protein was quantified by the method of Bradford (*24*), using HSA as a standard. FVIII activity was measured by a spectrophotometric assay using bovine coagulation factors (Coatest FVIII, Chromogenix AB, Mölndal, Sweden). The amount of FVIII in 1 mL of human plasma (1 unit/mL) was assumed to correspond to 0.35 nM. The concentration of FIXa was determined by active-site titration with antithrombin (*20*).

Mutagenesis and Construction of Expression Vectors. The mammalian expression vector pKG5 containing human FIX cDNA (*25*) was used as a template to construct full-length cDNAs encoding des-(N264,K265)-FIX and FIX-K265A. Mutagenesis was performed by a polymerase chain reaction-based method, using the oligonucleotide primers 5′-GTC CAG TTC TAG AAG GGC AAT GTC ATG GTT GTA AAT AGC TGC ATT GTA GTT-3′ [des-(N264,K265)-FIX] and 5′-GTC CAG TTC TAG AAG GGC AAT GTC ATG GTT GTA CGC ATT AAT AGC TGC ATT-3′ (FIX-K265A). A restriction site for *Xba*I was introduced by silent mutagenesis to facilitate further cloning (underlined). The mutated FIX cDNA fragments were digested and subsequently ligated into the pKG5 vector. The final FIX cDNAs were verified by DNA sequencing.

Recombinant FIX. Madin−Darby canine kidney (MDCK) cells were grown in DMEM supplemented with 10% FCS. Transfection of MDCK cells with expression vector pKG5 containing FIX cDNA was performed using the calcium phosphate coprecipitation method. Stable cell lines producing the different FIX molecules were obtained as described (*26*). Production of FIX antigen was assayed by enzyme-linked immunosorbent assay. Cell lines producing appropriate amounts of FIX were selected for large-scale production in 1 L cell factories as described previously (*27*). As established previously, recombinant FIX produced by this expression system is indistinguishable from plasma-derived FIX with

Table 2: Hydrolysis of Various Amide Substrates by Normal and Mutant FIXa[a]

	pNA formation (μM·min^{-1})		
	normal FIXa	des-(N264,K265)-FIXa	FIXa-K265A
CH_3SO_2-Leu-Gly-Arg-pNA	6.6 ± 0.1	6.3 ± 0.1	14.7 ± 0.4
CH_3OCO-CHG-Gly-Arg-pNA	8.2 ± 0.1	7.1 ± 0.2	17.0 ± 0.3
CH_3OCO-CHG-NVal-Arg-pNA	2.1 ± 0.1	4.3 ± 0.1	8.3 ± 0.1
H-CHG-NVal-Arg-pNA	1.0 ± 0.1	2.3 ± 0.1	5.0 ± 0.2
CH_3OCO-CHT-NVal-Arg-pNA	1.2 ± 0.1	2.7 ± 0.2	4.5 ± 0.2

[a] Activity toward various amide substrates was assayed as described under Experimental Procedures. Final concentrations of FIXa and substrate were 75 nM and 1 mM, respectively. Values represent the mean ± SD of four experiments.

respect to barium citrate adsorption and binding to a Ca^{2+}-dependent monoclonal antibody directed against the Gla domain (*27*). Furthermore, similar activities are found for recombinant wild-type and plasma-derived FIXa (*27*). These observations are consistent with previous reports that established normal γ-carboxylation of FIX produced by this expression system (*25*, *28*). Purification of recombinant FIX from concentrated medium was performed using the same immunopurification procedure as described previously (*27*). The activated forms of recombinant and plasma-derived FIX were obtained by incubation of FIX with human FXIa as outlined previously (*20*). FIXaβ was purified from the activation mixture employing anion exchange chromatography as described (*20*).

Amidolytic Activity. Hydrolysis of amide substrates was assayed in 30% (v/v) ethylene glycol, 0.2 mg/mL HSA, 0.1 M NaCl, 5 mM $CaCl_2$, 0.05 M Tris (pH 7.4) at 37 °C. Initial rates of substrate hydrolysis were determined at an enzyme concentration of 75 nM. Absorbance values were converted into molar concentrations using a molar extinction coefficient of 9650 M^{-1} cm^{-1} for pNA and a path length of 0.35 cm for a 100 μL volume. The catalytic efficiency for CH_3SO_2-LGR-pNA hydrolysis was determined in the absence of ethylene glycol as outlined previously (*10*).

FX Activation. FX activation was assayed as described previously (*29*). Briefly, phospholipid vesicles (50% phosphatidylserine, 50% phosphatidylcholine) and calcium ions were preincubated for 10 min, before the sequential addition of FX and FIXa. FXa formation was stopped by addition of EDTA (0.01 M final concentration) and subsequently quantified employing the chromogenic substrate S2222 (Chromogenix AB, Mölndal, Sweden). The relation between S2222 hydrolysis and FXa concentration was determined by using an active site-titrated FXa reference preparation. During the activation period, less than 5% of FX was converted, and FXa formation was linear in time. FVIII-dependent activation of FX was addressed by the addition of unactivated FVIII to a mixture of phospholipids (0.1 mM), FIXa (0.1 nM), and thrombin (5 nM). After 1 min of incubation, FXa formation was initiated by the addition of FX. FXa generation was quantified as described above, and initial rates were calculated from the increase in FXa concentration during the first 2 min of incubation.

Slow-Binding Kinetics. Inhibition of mutant and normal FIXa by antithrombin was measured using the slow-binding kinetic approach, as outlined previously (*30*, *10*). A series of inhibition progress curves was generated at 37 °C using 10 nM FIXa, 2.5 mM CH_3SO_2-LGR-pNA, and varying concentrations of antithrombin (0−1.5 μM). In the presence of cofactor, FIXa was preincubated with intact FVIIIa (final concentration 20 nM) and phospholipid vesicles (final concentration 50 μM) or isolated FVIII A2 domain (final concentration 135 nM) and subsequently added to the reaction mixture containing antithrombin and CH_3SO_2-LGR-pNA. The apparent first-order rate constant (k') was obtained for each antithrombin concentration by fitting the data from the progress curves to the integrated rate equation for slow binding (*30*). A plot of k' versus the inhibitor concentration yields the association and dissociation rate constants (k_{ass} and k_{dis}), according to eq 2 in ref *10*.

RESULTS

Recombinant Proteins. To investigate the contribution of insertion loop 256−268 to human FIX function, variants FIX-K265A and des-(N264,K265)-FIX were constructed. In FIX-K265A, Lys^{265} was replaced by the small and neutral amino acid Ala. In the des-(N264,K265)-FIX variant, the size of loop 256−268 was reduced to that of related coagulation proteases (see Table 1). Both FIX variants were expressed in MDCK cells and purified from the culture medium by immunoaffinity chromatography as described under Experimental Procedures. Both mutants could be converted completely to FIXaβ by FXIa, and the conversion rate was similar to that of normal FIX. The final preparations of mutant and normal FIXa were more than 90% active as assessed by active site titration with antithrombin.

Amidolytic Activity. The potential role of loop 256−268 in FIXa activity was examined first by measuring the reactivity of FIXa-K265A, des-(N264,K265)-FIXa, and normal FIXa toward the synthetic substrate CH_3SO_2-LGR-pNA. Initial rates of *p*-nitroanilide formation at various substrate concentrations were used to calculate the catalytic efficiency (k_{cat}/K_m) for normal and mutant FIXa. The k_{cat}/K_m values (mean ± SD) were 4.2 (±0.3) × 10^2, 5.0 (±0.2) × 10^2 and 1.9 (±0.1) × 10^2 M^{-1}·s^{-1} for FIXa-K265A, des-(N264,K265)-FIXa, and normal FIXa, respectively. Thus, the mutations in surface loop 256−268 promote the activity of FIXa toward the amide substrate CH_3SO_2-LGR-pNA.

This increase in amidolytic activity was investigated in more detail by measuring the activity of mutant and normal FIXa toward a series of closely related amide substrates (see Table 2). Due to limited solubility of the substrates with NVal in P2, these experiments were performed in the presence of 30% ethylene glycol and at a fixed substrate concentration of 1 mM. Under these conditions, des-(N264,K265)-FIXa displayed almost the same reactivity toward substrates with Gly in P2 as normal FIXa, while the activity of FIXa-K265A was approximately 2-fold higher. Substrates with NVal in this position were cleaved less efficiently by both normal and mutant FIXa. However, the reduction in reactivity toward

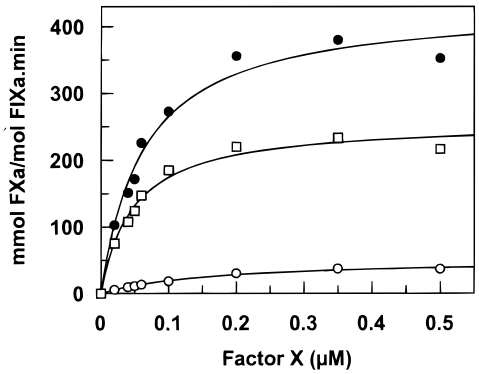

FIGURE 1: FX activation by mutant and normal FIXa in the absence of FVIIIa. Various concentrations of FX (0−0.5 μM) were incubated in 5 mM $CaCl_2$, 0.1 M NaCl, 0.2 mg/mL HSA, 0.05 M Tris (pH 7.4) with 30 nM of normal FIXa (open circles), des-(N264,K265)-FIXa (open squares), or FIXa-K265A (closed circles) in the presence of 0.1 mM phospholipid vesicles. FXa formation was quantified as described under Experimental Procedures. The apparent K_m and k_{cat} values for normal FIXa were 0.17 (±0.02) μM and 52 (±3) × 10^{-3} min^{-1}, respectively. The apparent K_m for des-(N264,K265)-FIXa was 0.05 (±0.01) μM, and the apparent k_{cat} was 257 (±10) × 10^{-3} min^{-1}. For FIXa-K265A, the apparent K_m was 0.06 (±0.01) μM, and the apparent k_{cat} was 433 (±21) × 10^{-3} min^{-1}. Data represent mean values of four independent experiments.

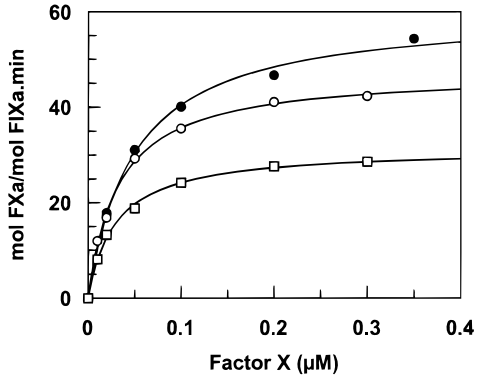

FIGURE 2: FVIIIa-dependent activation of FX by normal and mutant FIXa. Various concentrations of FX (0−0.35 μM) were incubated with 0.1 nM of normal FIXa (open circles), des-(N264,K265)-FIXa (open squares), or FIXa-K265A (closed circles) in the presence of 0.1 mM phospholipid vesicles and 0.35 nM FVIIIa in 5 mM $CaCl_2$, 0.1 M NaCl, 0.2 mg/mL HSA, 0.05 M Tris (pH 7.4). FXa formation was quantified as described under Experimental Procedures. The apparent K_m and k_{cat} values for normal FIXa were 0.03 (±0.01) μM and 47.3 (±2.3) min^{-1}, respectively. The apparent K_m for des-(N264,K265)-FIXa was 0.03 (±0.01) μM, and the apparent k_{cat} was 31.4 (±1.8) min^{-1}. For FIXa-K265A, the apparent K_m was 0.05 (±0.02) μM, and the apparent k_{cat} was 60.2 (±5.4) min^{-1}. Data represent mean values of multiple independent experiments.

these substrates was more pronounced for normal FIXa than for des-(N264,K265)-FIXa and FIXa-K265A (Table 2). Variation of the P3 residue or the blocking group had a similar effect on the amidolytic activity of mutant and normal FIXa. Collectively, these findings suggest that mutation of residues Asn^{264}−Lys^{265} enhances the hydrolysis of tripeptide substrates mainly by influencing the interactions in the S2 binding site.

The amidolytic activity of normal and mutant FIXa was also assessed in the presence of FVIIIa. To this end, varying concentrations of CH_3SO_2-LGR-pNA (0−5 mM) were incubated with FIXa (50 nM) in the presence of FVIIIa (50 nM) and phospholipid vesicles (50 μM). Under these conditions, the k_{cat}/K_m values for cleavage of CH_3SO_2-LGR-pNA by FIXa-K265A, des-(N264,K265)-FIXa, and normal FIXa were, respectively, 103%, 104%, and 108% of those in the absence of cofactor. Apparently, the amidolytic activities of both normal and mutant FIXa remain unaltered upon addition of FVIIIa.

FX Activation in the Absence of FVIIIa. As both FIXa variants displayed increased reactivity toward the synthetic substrate CH_3SO_2-LGR-pNA, it was of interest to investigate the enzymatic activity toward the physiological substrate FX. In these experiments, FXa generation by mutant and normal FIXa was measured in the presence of phospholipid vesicles, calcium ions, and various concentrations of FX. As shown in Figure 1, FX activation by FIXa-K265A and des-(N264,-K265)-FIXa was strongly increased in comparison with normal FIXa. Both mutants displayed significantly lower apparent K_m values (0.05−0.06 μM versus 0.17 μM for normal FIXa). The reduction in apparent K_m was accompanied by an increase in apparent k_{cat} for both FIXa variants. Consequently, the catalytic efficiencies (apparent k_{cat}/K_m) of FX activation were approximately 20-fold higher than that of normal FIXa. This demonstrates that residues 264 and 265 in surface loop 256−268 limit the proteolytic activity of FIXa toward FX.

FX Activation in the Presence of FVIIIa. Activation of FX was also assessed in the presence of the physiological cofactor FVIIIa. To this end, FXa generation by mutant and normal FIXa was measured in the presence of 0.35 nM FVIIIa and various FX concentrations. Strikingly, FVIIIa-dependent activation of FX was only slightly increased for FIXa-K265A compared to normal FIXa, while the reactivity of des-(N264,K265)-FIXa toward FX was even lower than that of normal FIXa (Figure 2). The combination of increased proteolytic activity toward FX in the absence of FVIIIa and close to normal activity in the presence of this cofactor endowed the FIXa variants with reduced FVIIIa stimulation relative to normal FIXa. The factor VIIIa stimulation factor, defined as the ratio of k_{cat}/K_m toward FX in the presence and absence of FVIIIa, was approximately 5100 for normal FIXa, while FVIIIa enhanced the enzymatic activity of des-(N264,K265)-FIXa and FIXa-K265A only 180-fold.

It has been demonstrated previously that FIXa is able to inactivate FVIIIa by proteolytic cleavage at Arg^{336} in the A1 domain (*31*, *32*). One explanation for the reduced FVIIIa stimulation would therefore be that the two FIXa variants inactivate FVIIIa more rapidly than normal FIXa. To investigate this possibility, we incubated FVIIIa with FIXa-K265A or normal FIXa in the presence of phospholipids and analyzed FVIIIa proteolysis in time by SDS−PAGE. As shown in Figure 3, both enzymes cleaved the A1 domain of FVIIIa at a similar rate, indicating that the mutations in surface loop 256−268 have no effect on the FIXa-catalyzed proteolysis of FVIIIa. Furthermore, the time courses of FX activation in the presence of FVIIIa (0.35 nM) revealed that the first-order rate constant for the decline in cofactor-dependent activity was 0.5 ± 0.1 min^{-1} for normal and mutant FIXa. It has been well established that this decline originates from inactivation of FVIIIa (*33*, *34*), and therefore these results provide additional evidence that the reduction in FVIIIa stimulation is not due to an increase in the FIXa-dependent inactivation of FVIIIa.

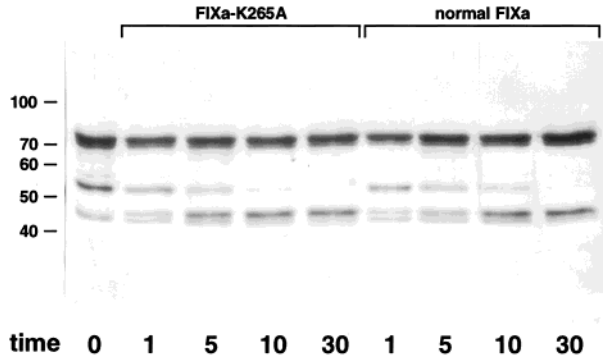

FIGURE 3: FVIIIa proteolysis by normal FIXa and FIXa-K265A. FVIIIa (250 nM) was incubated with 50 nM FIXa-K265A (left section) or normal FIXa (right section) in the presence of 0.1 mM phospholipid vesicles in 0.1 M NaCl, 10 mM $CaCl_2$, 0.05 M Tris (pH 7.4) at 37 °C. At the times indicated in minutes, aliquots were removed from the incubation mixture and subjected to SDS−PAGE under reducing conditions using a 10% gel. Proteins were visualized by silver staining. Positions of molecular mass standards (in kDa) are indicated on the left.

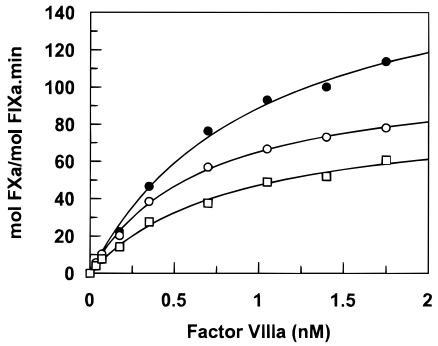

FIGURE 4: Comparison of the apparent affinity of mutant and normal FIXa for FVIIIa. FX (0.2 μM) was incubated with 0.1 nM of normal FIXa (open circles), des-(N264,K265)-FIXa (open squares), or FIXa-K265A (closed circles) in the presence of 0.1 mM phospholipid vesicles with various concentrations of FVIIIa (0−1.75 nM) in 5 mM $CaCl_2$, 0.1 M NaCl, 0.2 mg/mL HSA, 0.05 M Tris (pH 7.4). FXa formation was quantified as described under Experimental Procedures. Data represent mean values of three independent experiments. The apparent K_d values were 0.7 (±0.1), 0.7 (±0.1), and 1.0 (±0.1) nM for normal FIXa, des-(N264,K265)-FIXa, and FIXa-K265A, respectively.

Another explanation for the reduction in FVIIIa stimulation would be that mutation of the Asn^{264}−Lys^{265} motif results in a lower affinity for FVIIIa. To test this hypothesis, we addressed FX activation in the presence of various FVIIIa concentrations. As shown in Figure 4, FVIIIa enhanced FX conversion by normal and mutant FIXa in a saturable and dose-dependent manner. The apparent K_d values for FVIIIa binding, derived from the kinetics of FX activation, were 0.7 (±0.1), 1.0 (±0.1), and 0.7 (±0.1) nM for des-(N264,-K265)-FIXa, FIXa-K265A, and normal FIXa, respectively. Thus, mutagenesis of loop 256−268 has little, if any, effect on the affinity for FVIIIa. Collectively, these data demonstrate that both FIXa variants display a reduced response to FVIIIa, while the affinity for this cofactor and the FIXa-dependent inactivation of FVIIIa remain essentially unaltered.

Inhibition by Antithrombin. To further characterize the role of loop 256−268 in the interaction with macromolecular substrates, the inhibition of mutant and normal FIXa by the pseudosubstrate antithrombin was evaluated. To this end, inhibition experiments under slow-binding conditions (see Experimental Procedures) were performed, in which FIXa-K265A, des-(N264,K265)-FIXa, and normal FIXa were incubated with various concentrations of antithrombin and a competing chromogenic substrate. In Figure 5 the apparent first-order rate constant (k') obtained at each antithrombin concentration was plotted versus the inhibitor concentration. As the chromogenic substrate concentration used in these experiments was much lower than the K_m for all three enzymes, the slope of each line directly represents the association rate constant (k_{ass}). The k_{ass} and k_{dis} values for the inhibition of mutant and normal FIXa by antithrombin are presented in Table 3. These data show that both FIXa variants displayed increased susceptibility to antithrombin inhibition, although the increase was less pronounced than that observed for FX activation. Apparently, insertion loop 256−268 also contributes to the interaction of FIXa with antithrombin.

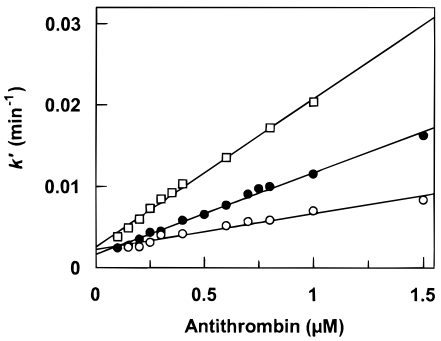

FIGURE 5: Inhibition of mutant and normal FIXa by antithrombin. Plot of k' versus the antithrombin concentration for normal FIXa (open circles), des-(N264,K265)-FIXa (open squares), and FIXa-K265A (closed circles). Data from slow-binding inhibition curves were fitted to the integrated rate equation for slow binding (*29*), and values for k' were obtained at each inhibitor concentration. The slope of each line represents the k_{ass}, while k_{dis} is equal to the y intercept.

Table 3: Kinetic Constants for Antithrombin Inhibition of Mutant and Normal FIXa[a]

	$k_{ass} \times 10^{-3}$ (M^{-1}·min^{-1})	$k_{dis} \times 10^{3}$ (min^{-1})
normal FIXa	4.4 ± 0.3	2.2 ± 0.2
des-(N264,K265)-FIXa	18.2 ± 0.4	2.6 ± 0.2
FIXa-K265A	10.0 ± 0.1	1.6 ± 0.2

[a] The k_{ass} and k_{dis} values for inhibition of des-(N264,K265)-FIXa, FIXa-K265A, and normal FIXa by antithrombin were derived from the data in Figure 5 as described under Experimental Procedures.

The same kinetic approach was used to investigate the influence of FVIIIa on the inhibition of normal and mutant FIXa by antithrombin. As the cofactor activity of FVIIIa decays rapidly in time, only the initial phase of the inhibition progress curves was analyzed. Comparison of these data with those obtained in the absence of cofactor revealed that FVIIIa has no significant effect on the inhibition of normal or mutant FIXa by antithrombin (data not shown). The interaction with antithrombin was further explored in the presence of the isolated FVIII A2 domain. This subunit has been shown to enhance the FIXa-catalyzed activation of FX, although to a much lesser extent than intact FVIIIa (*23*). The k_{ass} and k_{dis} values for antithrombin inhibition in the presence of A2 subunit varied between 80 and 120% of those in the absence of cofactor for both normal and mutant FIXa. Thus, under the conditions used in these experiments, neither FVIIIa nor

its isolated A2 subunit affected the interaction of normal or mutant FIXa with antithrombin. In control experiments, isolated A2 domain (100 nM) was found to stimulate the conversion of FX by normal FIXa approximately 30-fold, which is consistent with published data (*23*).

DISCUSSION

The enzymes involved in blood coagulation bear marked similarity to the serine proteases trypsin and chymotrypsin both in amino acid sequence and in three-dimensional structure. However, unlike trypsin and chymotrypsin, the coagulation proteases display high specificity for a limited number of substrates. In addition, the majority of the coagulation enzymes exhibit low intrinsic activity toward their natural substrates and require protein cofactors for full biological function. The variations in specificities and activities among the various serine proteases are believed to arise from structural differences in surface loops that border their substrate-binding grooves (*35*, *36*). In particular, insertions in surface loops near the active site have been shown to play a major role in modulating the reactivity toward substrates and inhibitors (*10*−*13*). In the present study, we investigated the functional role of insertion loop 256−268, and in particular of the Asn^{264}−Lys^{265} motif therein, by characterizing the mutants FIXa-K265A and des-(N264,K265)-FIXa.

FX activation studies in the absence of FVIIIa demonstrated that the proteolytic activity of both FIXa mutants toward FX was strongly increased compared to that of normal FIXa (Figure 1). Determination of the catalytic parameters for this reaction revealed that this increase was due to a combination of reduced K_m and increased k_{cat}. These data suggest that in normal FIXa loop 256−268 interferes not only with the binding of FX in the substrate-binding groove but also with the subsequent hydrolysis of the FX scissile bond. By doing so, loop 256−268 restricts the enzymatic activity of FIXa in the absence of its cofactor FVIIIa. The low activity of FIXa and related coagulation enzymes in the absence of their respective cofactors constitutes an important regulatory mechanism in maintaining the hemostatic balance. The mutations in loop 256−268 also promoted the inhibition by FIXa's primary physiological inhibitor antithrombin, although the increase was less pronounced than that observed for FX activation. The enhancement of antithrombin inhibition was due to a 2−4-fold increase in k_{ass}, whereas the k_{dis} remained essentially unchanged (Table 3).

Besides promoting the reactivity toward the macromolecular substrates FX and antithrombin, mutation of residues Asn^{264}−Lys^{265} also enhanced FIXa activity toward various amide substrates. This enhancement of amidolytic activity was less pronounced than that observed for the chimeric FIXa variant in which loop region 260−265 was exchanged for the corresponding region of FX (*14*). In the latter variant, however, the deletion of the Asn^{264}−Lys^{265} motif was combined with the introduction of four residues of FXa, an enzyme with much higher amidolytic activity than FIXa. It may be noted that the amidolytic activity of normal and mutant FIXa toward the various tripeptide substrates (Table 2) was determined in the presence of ethylene glycol, which is known to enhance the amidolytic activity of FIXa by an as yet unknown mechanism (*37*). The observation that ethylene glycol stimulated the amidolytic activity of normal FIXa and FIXa-K265A to a larger extent than that of des-(N264,K265)-FIXa (10-fold versus 3-fold) may suggest that the potentiating effect of ethylene glycol involves this surface region.

It has been shown for a number of serine proteases that residues located in surface loop *c*91−101 are involved in substrate binding. For example, a cluster of four basic residues present in the equivalent surface loop of enteropeptidase makes ionic contacts with acidic residues in the P2−P5 positions of the trypsinogen substrate (*38*). In the present study, we showed that the difference in amidolytic activity between the two FIXa variants and normal FIXa was more pronounced for substrates with NVal at P2 than with Gly at this position (Table 2). In addition, the enzymatic activity toward FX (Thr at P2) was increased approximately 20-fold for both FIXa variants, whereas the susceptibility to antithrombin inhibition (Gly at P2) was only 3-fold increased. Together, these findings indicate that mutation of residues Asn^{264}−Lys^{265} improves the ability of FIXa to accommodate substrate residues with relatively large side chains in the S2 binding site. As already noted by Hopfner et al. (*16*), the two-residue insertion in surface loop 256−268 of FIXa has a considerable effect on the conformation of this loop region. The most striking difference within this region between FIXa and related serine proteases is the orientation of the side chain of residue *c*99 (Tyr^{266} in FIXa). In the absence of substrate interactions, this side chain seems to block the S2 site, as predicted by the three-dimensional structure of human FIXa in complex with *p*-aminobenzamidine (*16*). The structure of porcine FIXa in complex with the substrate analogue D-Phe-Pro-Arg-chloromethyl ketone (*15*) reveals that the side chain of Tyr^{266} adopts a different conformation upon substrate binding, which results in the formation of the S2 site but at the same time restricts the accessibility to the S4 binding site (Figure 6). Results from our present study together with the above-mentioned structural data support a model in which mutation of residues Asn^{264}−Lys^{265} induces or allows a different conformation of surface loop 256−268 that makes the position of the Tyr^{266} side chain less unfavorable with respect to substrate residues at P2. However, we cannot fully exclude the possibility that mutation of Asn^{264}−Lys^{265} directly affects the interactions in the S2 site since the side chain of Lys^{265} is located within close proximity to the P2 residue of D-Phe-Pro-Arg-chloromethyl ketone (Figure 6).

FX activation experiments in the presence of FVIIIa revealed that the enzymatic activity of normal FIXa was stimulated to a larger extent than that of FIXa-K265A and des-(N264,K265)-FIXa, resulting in similar activities for all three enzymes (Figure 2). This difference in FVIIIa enhancement between normal and mutant FIXa was neither due to a difference in FIXa-dependent inactivation of FVIIIa nor due to a difference in binding affinity for this cofactor (Figures 3 and 4). Determination of the kinetic parameters of FX activation revealed that the two FIXa variants display similar K_m values in the absence and presence of FVIIIa, whereas the K_m for normal FIXa was 5 times decreased upon addition of FVIIIa. These findings are consistent with a model in which obstruction of the S2 binding site by the Tyr^{266} side chain, that occurs in normal FIXa but probably not in the two FIXa variants, is abolished when FIXa binds to FVIIIa. Recently, we have demonstrated that FIXa activity toward

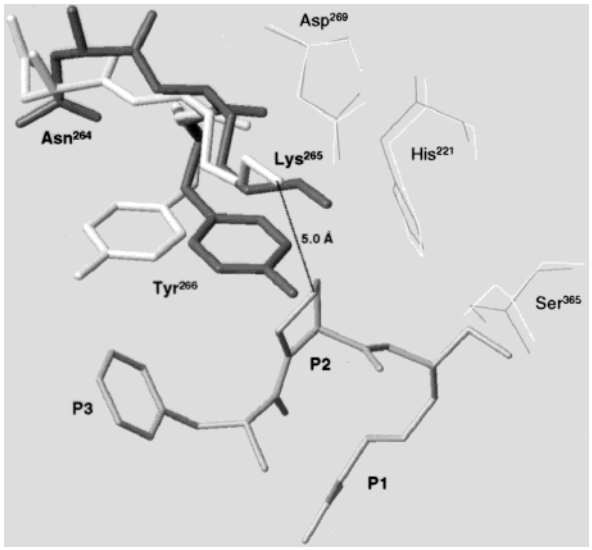

FIGURE 6: Comparison of the side chain conformations in loop segment Asn^{264}−Tyr^{266} of porcine FIXa in complex with D-Phe-Pro-Arg-chloromethyl ketone (*15*) and human FIXa inhibited with *p*-aminobenzamidine (*16*). Porcine FIX residues are shown in white, while residues of the human protein are depicted in black. The catalytic residues Ser^{365}, His^{221}, and Asp^{269} of both FIXa species are also shown. The side chain of Lys^{265} is located within 5 Å of the P2 Pro of D-Phe-Pro-Arg-chloromethyl ketone (gray). Residues Phe, Pro, and Arg of D-Phe-Pro-Arg-chloromethyl ketone are labeled P3, P2, and P1, respectively.

FX is severely impaired when surface loop 199−204 is exchanged for the corresponding region of related coagulation factors. This reduction in proteolytic activity, however, was largely restored upon complex formation with FVIIIa (*10*). Together, these observations suggest that FVIIIa induces structural rearrangements in the surface loops that surround FIXa's active site region, thereby alleviating unfavorable interactions between these loops and the FX substrate. This view is in agreement with a previous study demonstrating that binding of FVIIIa modifies the environment of a fluorescent probe that was covalently attached to the active site of FIXa (*39*). The rearrangements in FIXa's surface loops are likely to play an important role in the FVIIIa-dependent enhancement of FX activation. Unlike the activation of FX, cleavage of amide substrates is not accelerated in the presence of FVIIIa (this study and refs *7*, *8*). In this regard, it is important to note that for the conversion of FX by FIXa acylation is rate-limiting and that binding of FVIIIa accelerates this reaction step (*40*). In contrast, for the hydrolysis of oligopeptide amide substrates, deacylation is most likely the rate-limiting step (*41*, *42*). This notion would explain why FVIIIa has no effect on FIXa's amidolytic activity. Finally, it should be noted that the FX substrate binds to FVIIIa in the FX-activating complex via an interactive site in the A1 domain of FVIII (*43*, *44*). This interaction in combination with the above-mentioned surface loop rearrangements may accomplish the stimulatory effect of FVIIIa on FX activation.

REFERENCES

1. Stenflo, J. (1991) *Blood 78*, 1637−1651.
2. Furie, B., and Furie, B. C. (1988) *Cell 53*, 505−518.
3. Davie, E. W., Fujikawa, K., and Kisiel, W. (1991) *Biochemistry 30*, 10363−10370.
4. Mann, K. G., Nesheim, M. E., Church, W. R., Haley, P., and Krishnaswamy, S. (1990) *Blood 76*, 1−16.
5. van Dieijen, G., Tans, G., Rosing, J., and Hemker, H. C. (1981) *J. Biol. Chem. 256*, 3433−3442.
6. Mertens, K., van Wijngaarden, A., and Bertina, R. M. (1985) *Thromb. Haemostasis 54*, 654−660.
7. Castillo, M. J., Kurachi, K., Nishino, N., Ohkubo, I., and Powers, J. C. (1983) *Biochemistry 22*, 1021−1029.
8. Chang J., Jin, J., Lollar, P., Bode, W., Brandstetter, H., Hamaguchi, N., Straight, D. L., and Stafford, D. W. (1998) *J. Biol. Chem. 273*, 12089−12094.
9. Kolkman, J. A., Lenting, P. J., and Mertens, K. (1999) *Biochem. J. 339*, 217−221.
10. Kolkman, J. A., Christophe, O. D., Lenting, P. J., and Mertens, K. (1999) *J. Biol. Chem. 274*, 29087−29093.
11. Le Bonniec, B. F., Guinto, E. R., MacGillivray, R. T., Stone, S. R., and Esmon, C. T. (1993) *J. Biol. Chem. 268*, 19055−19061.
12. Le Bonniec, B. F., Guinto, E. R., and Esmon, C. T. (1992) *J. Biol. Chem. 267*, 19341−19348.
13. Madison, E. L., Goldsmith, E. J., Gerard, R. D., Gething, M.-J. H., and Sambrook, J. F. (1989) *Nature 339*, 721−724.
14. Hopfner, K.-P., Brandstetter, H., Karcher, A., Kopetzki, E., Huber, R., Engh, R. A., and Bode, W. (1997) *EMBO J. 16*, 6626−6635.
15. Brandstetter, H., Bauer, M., Huber, R., Lollar, P., and Bode, W. (1995) *Proc. Natl. Acad. Sci. U.S.A. 92*, 9796−9800.
16. Hopfner, K.-P., Lang, A., Karcher, A., Sichler, K., Kopetzki, E., Brandstetter, H., Huber, R., Bode, W., and Engh, R. A (1999) *Structure 7*, 989−996.
17. Sarkar, G., Koeberl, D. D., and Sommer, S. S. (1990) *Genomics 6*, 133−143.
18. Lenting, P. J., van de Loo, J. W. P. H., Donath, M. J. S. H., van Mourik, J. A., and Mertens, K. (1996) *J. Biol. Chem. 271*, 1935−1940.
19. Lenting, P. J., Donath, M. J. S. H., van Mourik, J. A., and Mertens, K. (1994) *J. Biol. Chem. 269*, 7150−7155.
20. Lenting, P. J., ter Maat, H., Clijsters, P. P. F. M., Donath, M. J. S. H., van Mourik, J. A., and Mertens, K. (1995) *J. Biol. Chem. 270*, 14884−14890.
21. Mertens, K., Cupers, R., van Wijngaarden, A., and Bertina, R. M. (1984) *Biochem. J. 223*, 599−605.
22. Curtis, J. E., Helgerson, S. L., Parker, E. T., and Lollar, P. (1994) *J. Biol. Chem. 269*, 6246−6251.
23. Fay, P. J., and Koshibu, K. (1998) *J. Biol. Chem. 273*, 19049−19054.
24. Bradford, M. M. (1976) *Anal. Biochem. 72*, 248−254.
25. Rees, D. J. G., Jones, I. M., Handford, P. A., Walter, S. J., Esnouf, M. P., Smith, K. J., and Brownlee, G. G. (1988) *EMBO J. 7*, 2053−2061.
26. Christophe, O. D., Lenting, P. J., Kolkman, J. A., Brownlee, G. G., and Mertens, K. (1998) *J. Biol. Chem. 273*, 222−227.
27. Lenting, P. J., Christophe, O. D., ter Maat, H., Rees, D. J. G., and Mertens, K. (1996) *J. Biol. Chem. 271*, 25332−25337.
28. Hughes, P. E., Handford, P. A., Austen, D. E. G., and Brownlee, G. G. (1994) *Protein Eng. 7*, 1121−1127.
29. Mertens, K., and Bertina, R. M. (1984) *Biochem. J. 223*, 607−615.
30. Morrison, J. F., and Walsh, C. T. (1988) *Adv. Enzymol. Relat. Areas Mol. Biol. 61*, 201−301.
31. Lamphear, B. J., and Fay. P. J. (1992) *Blood 80*, 3120−3126.
32. O'Brien, D. P., Johnson, D., Byfield, P., and Tuddenham, E. G. D. (1992) *Biochemistry 31*, 2805−2812.
33. Brinkman, H-.J., Koster, P., Mertens, K., and van Mourik, J. A. (1997) *Biochem. J. 323*, 735−740.
34. Fay, P. J., Beattie, T. L., Regan, L. M., O'Brien, L. M., and Kaufmann, R. J. (1996) *J. Biol. Chem. 271*, 6027−6032.
35. Bode, W., Brandstetter, H., Mather, T., and Stubbs, M. T. (1997) *Thromb. Haemostasis 78*, 501−511.
36. Perona, J. J., and Craik, C. S. (1997) *J. Biol. Chem. 272*, 29987−29990.
37. Sturzebecher, J., Kopetzki, E., Bode, W., and Hopfner, K.-P. (1997) *FEBS Lett. 412*, 295−300.
38. Matsushima, M., Ichinose, M., Yahagi, N., Kakei, N., Tsukada, S., Miki, K., Kurokawa, K., Tashiro, K., Shiokawa, K.,

Shinomiya, K., Umeyama, H., Inoue, H., Takahashi, T., and Takahashi, K. (1994) *J. Biol. Chem. 269*, 19976−19982.
39. Mutucumarana, V. P., Duffy, E. J., Lollar, P., and Johnson, A. E. (1992) *J. Biol. Chem. 267*, 17012−17021.
40. Duffy, E. J., and Lollar, P. (1992) *J. Biol. Chem. 267*, 7821−7827.
41. Hedstrom, L., Szilagyi, L., and Rutter, W. J. (1992) *Science 255*, 1249−1253.
42. Stein, R. L., Strimpler, A. M., Hori, H., and Powers, J. C. (1987) *Biochemistry 26*, 1301−1305.
43. Lapan, K. A., and Fay, P. J. (1997) *J. Biol. Chem. 272*, 2082−2088.
44. Lapan, K. A., and Fay, P. J. (1998) *Thromb. Haemostasis 80*, 418−422.

BI992735Q